

Systematics of Coulomb-Distortion Effects in Large-Angle $M1$ Electroexcitation*

B. T. CHERTOK†

Department of Physics, The American University, Washington, D. C. 20016

(Received 3 June 1969)

Computer calculations of inelastic electron scattering for $M1$ transitions in light nuclei are carried out for very low-energy electrons, $E_0 < 5$ MeV, and low-energy electrons $10 < E_0 < 70$ MeV. The calculation is a partial-wave analysis using the Duke program. Computer results are presented graphically as the Coulomb distortion versus Z , E_0 , k , and θ . The dependence of the assumed nuclear model on the calculation is examined. Numerical results are presented leading to a revision of the radiative width Γ_0 for the 15.1-MeV state of ^{12}C . Revised widths are presented for other $M1$ transitions in ^{10}B , ^{26}Mg , and ^{28}Si . With regard to the ^{12}C width, the present status of the conserved-vector-current test in ^{12}B , ^{12}C , and ^{12}N is discussed. Finally, the numerical significance of Coulomb effects in the $M1$ breakup of the deuteron by electrons with $E_0 < 100$ MeV is presented. The small Coulomb-distortion effect is compared with estimates of meson exchange currents in $\text{D}(e, e')np$.

1. INTRODUCTION

INELASTIC electron scattering has been a useful tool in nuclear physics for exploring nuclear transition currents.^{1,2} These currents have been extracted from the measured scattering by use of Born-approximation calculations. However, without a distorted-wave Born approximation (DWBA) or partial-wave-analysis calculation of the electron scattering, the measurements are of limited use in understanding nuclear physics in detail.³ In earlier studies of medium-weight nuclei at electron energies of 1–4 MeV, we observed a factor-of-10 increase due to Coulomb-distortion effects for $M1$ electroexcitation and 2–5 increase for $E2$ near excitation threshold.⁴ In this paper the low- Z region will be examined for both very low electron energies ($E_0 \geq k$) and low-energy inelastic electron scattering extending to about 70 MeV. By Coulomb effects we mean the distortion of the electron waves in the static nuclear Coulomb field, so that Coulomb corrections are defined here as the ratio of the DWBA to plane-wave Born-approximation (PWBA) cross sections,

$$f_e = d\sigma(\text{DWBA})/d\sigma(\text{PWBA}). \quad (1)$$

One observes that the Coulomb corrections in inelastic electron scattering are not negligible compared to other effects and interactions of interest in physics. For example, in the area of magnetic dipole transitions which will be the focus of this paper, the Coulomb corrections will be seen to play a significant role in the eventual determination of meson exchange currents in electrodisintegration of the deuteron for electron

energies $E_0 < 100$ MeV. Further, the transition magnetic moment connecting the 15.1-MeV state with the ground state of ^{12}C is measured by inelastic electron scattering. The value of $\mu_{\text{tr}}(^{12}\text{C})$ provides the only clear experimental test in the isobaric triad ^{12}B , ^{12}C , and ^{12}N for the equivalence of the vector part of the weak interaction with the electromagnetic interaction through the conserved-vector-current (CVC) theory of Feynman and Gell-Mann. Finally, the giant $M1$ transitions in self-conjugate nuclei, which are prominent in large-angle inelastic electron scattering spectra, provide information on basic correlations in the ground-state wave function of $1p$, $2s$, and $1d$ nuclei. In particular one can “measure”, $\langle 00 | \sum_k l_k \cdot s_k | 00 \rangle$.⁵

An abundance of data are already available for inelastic electron scattering from light nuclei of $Z < 15$. The data have been interpreted in terms of the Born approximation. The Coulomb corrections may change the nuclear form factor for $M1$ transitions outside the quoted experimental error, and this change in $B(M1, q, I, I_f)$ is, in turn, magnified near the photon point. In the preliminary report on reanalysis of inelastic electron scattering measurements in the range $30 \leq E_0 \leq 70$ MeV from the giant states ^{12}C (15.1 MeV) and ^{28}Si (11.42 MeV), and a dominant fragment of the $M1$ strength in ^{26}Mg (10.63 MeV), the inclusion of Coulomb corrections reduced the radiative widths from 11% in ^{12}C to 27% in ^{28}Si .⁶

Partial-wave analysis of the elastic electron scattering cross sections have been in use for some years, and partial-wave analysis through the DWBA have been developed for inelastic electron scattering producing electric transitions. Analytic expressions have been derived for electric transitions obviating the need for partial-wave analysis.⁷ Recently, Tuan *et al.* have generalized the Duke calculation for electron scattering

* Research supported by the National Science Foundation.

† Guest worker, the National Bureau of Standards.

¹ W. Barber, *Ann. Rev. Nucl. Sci.* **12**, 1 (1962).

² T. de Forest and J. Walecka, *Advan. Phys.* **15**, 1 (1966).

³ T. Griffy, D. Onley, J. Reynolds, and L. Biedenharn, *Phys. Rev.* **128**, 833 (1962); D. Onley, T. Griffy, and J. Reynolds, *ibid.* **129**, 1689 (1963); and D. Onley, J. Reynolds, and L. Wright, *ibid.* **134**, B945 (1964).

⁴ B. Chertok and W. T. K. Johnson, *Phys. Rev.* **174**, 1525 (1968).

⁵ D. Kurath, *Phys. Rev.* **130**, 1525 (1963).

⁶ B. Chertok and W. T. K. Johnson, *Phys. Rev. Letters* **22**, 67 (1969); **22**, 265 (E) (1969).

⁷ T. Schucan, *Phys. Rev.* **171**, 1142 (1968).

inducting magnetic transitions,⁸ and Drechsel has introduced the critical question of dependence of nuclear models in these calculations.⁹ A systematic study of Coulomb-distortion effects in $M1$ excitation from light nuclei is presented here.

2. CALCULATION

The Duke calculation of inelastic electron scattering, which is based on partial-wave analysis, will be used. This Duke cross section is a DWBA calculation, where the nuclear excitation is treated through first-order perturbation theory while the electron waves are treated more exactly by partial-wave analysis in the static nuclear Coulomb field. Following earlier treatments of the problem,^{8,9} the radial matrix element for a magnetic transition of multipolarity L is

$$R^M(\kappa L \kappa') = (2L+1)ik \int_0^\infty \int_0^\infty i[L(L+1)]^{-1/2} \\ \times J_{L,L}(r_N) j_L(kr_<) h_L^{(1)}(kr_>) \\ \times [(\kappa + \kappa') (f_\kappa g_{\kappa'} + g_\kappa f_{\kappa'})] r_e^2 dr_e r_N^2 dr_N, \quad (2)$$

where κ and κ' are the Dirac quantum numbers for the initial and final state of the electron, $r_<$ and $r_>$ are, respectively, the lesser and greater of r_e and r_N , and the $f(r_e)$ and $g(r_e)$ are the radial parts of the eigenfunctions of the Dirac equation for a static Coulomb potential. In Eq. (2), $J_{L,L}(r_N)$ represents the radial part of the magnetic transition operator.

Tuan *et al.*⁸ generalized the Duke calculation for magnetic transitions by using just the convection-current part of the nuclear transition current operator. The nucleus is parametrized as an incompressible and

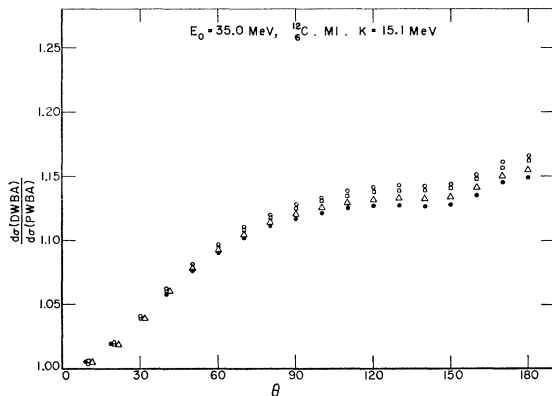


FIG. 1. Results of a computer calculation using the Duke program of inelastic electron scattering are presented. The model dependency of f_c versus electron scattering angle θ is shown. The input data for this $M1$ transition in ^{12}C are 10 partial waves, $Z=6$, $E_0=35.0$ MeV, and $k=15.1$ MeV; $c=2.38$ fm and $t=2.40$ fm are used in (4) and (3). The four sets of points refer to different $\rho_1(M1)$ in (3). \square : $t_{tr}/t=0.80$; \triangle : $t_{tr}/t=1.00$; \bullet : $t_{tr}/t=1.20$; and \diamond : $\rho_1(M1)=\rho_0$, with $t_{tr}/t=1.00$.

⁸ S. Tuan, L. Wright, and D. Onley, Nucl. Instr. Methods **60**, 70 (1968).

⁹ D. Drechsel, Nucl. Phys. **A113**, 665 (1968).

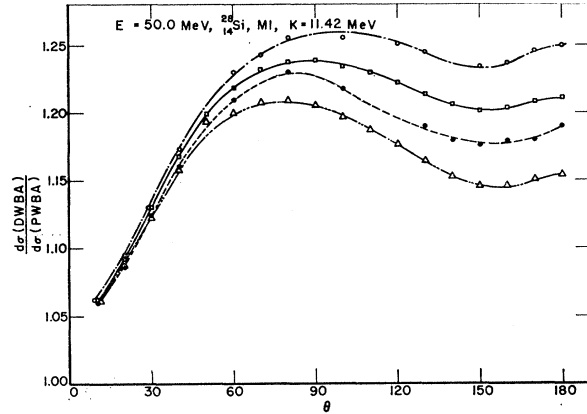


FIG. 2. As in Fig. 1, calculations of f_c are presented for the 11.42-MeV transition in ^{28}Si . $c=3.153$ fm and $t=2.40$ fm are used in (4) and (3). The four curves refer to models or parameters for the nuclear convection current $\mathbf{J}_N = \rho_1 \mathbf{Y}_{111}^{M*}$. These are, with ρ_1 defined in (3), \square : $t_{tr}/t=0.8$; \circ : $t_{tr}/t=1.0$; \triangle : $t_{tr}/t=1.2$; and \diamond : $t_{tr}/t=1.00$, with $\rho_1 = \rho_0$.

irrotational liquid drop assuming that the excited state resulting from a transition of multipolarity L has approximately the same shape as the ground state. They use $\mathbf{J}_N = \rho_1 \mathbf{Y}_{L,L,1}^M$, where

$$\rho_1(M1) = d\rho_0/dr \quad (3)$$

and ρ_0 , the Fermi charge distribution for the ground state, is

$$\rho_0 = \{1 + \exp[(r-c)/t]\}^{-1}. \quad (4)$$

The complete magnetic transition operator $\mathbf{J}_N + \nabla \times \boldsymbol{\mu}_N$ is not used since it is not yet clear, in general, whether the spin currents are uniformly distributed over the nuclear volume, very localized, or characterized by some superposition of uniform and localized magnetization. Progress is being made in parametrizing the operator $\mathbf{J}_N + \nabla \times \boldsymbol{\mu}_N$.¹⁰

The question of the dependency of the DWBA result on $J_{L,L}$ is critical. Reference is made to Table I in an earlier paper⁴ and to Figs. 1 and 2. Drechsel has already demonstrated that the model dependency of the Coulomb-distortion ratio $d\sigma(\text{DWBA})/d\sigma(\text{PWBA})$ in magnetic and transverse electric electroexcitation may be appreciable at large angles of $\theta \geq 100^\circ$.⁹ He computed the distortion ratio for $Z=28$, $E_0=50$ MeV for $M1$ transitions induced by the electron scattering, using several models for the transition operator $\mathbf{J}_N + \nabla \times \boldsymbol{\mu}_N$. Among other results he has demonstrated that the concept of a unique transition radius for magnetic transitions in nuclei is misleading and that it is simply a function of the specific model one assumes for the nuclear convection and spin currents.

The nuclear model used here, namely, convection currents near the nuclear surface [$\mathbf{J}_N = (d\rho_0/dr) \mathbf{Y}_{111}^{M*}$], yields Coulomb-distortion ratios for $Z=28$, $E_0=50$ MeV

¹⁰ H. Überall (private communication); H. Überall and P. Uginčius, Phys. Rev. **178**, 1565 (1969).

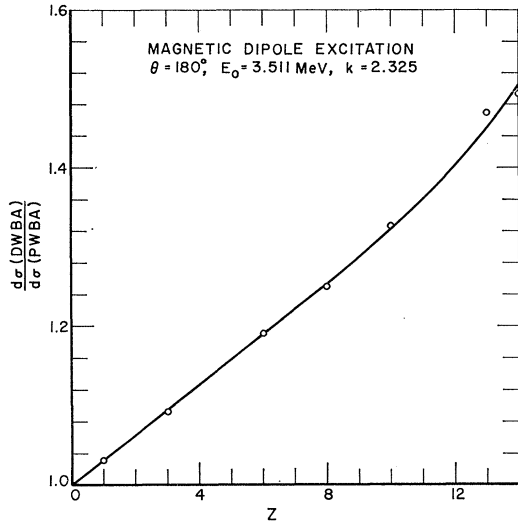


FIG. 3. Calculated $M1$ -distortion ratio versus atomic number for very low-energy electroexcitation at $\theta=180^\circ$ is shown. For $Z \leq 10$, the curve is linear, $f_e = 1 + 4.4Z\alpha$, $\alpha = 1/137$.

in good quantitative agreement with Drechsel's values for two models—which, he notes, are extreme tests of model independence. These latter models are $J_N \sim r \exp(-r/r_0) Y_{111}^{M*}$ and $\mu_N \sim \delta(R_A - r) Y_{101}^{M*} + c\delta(bR_A - r) Y_{121}^{M*}$. Since J_N is a continuous function and μ_N is discontinuous, in these cases the agreement of the distortion ratios $d\sigma(\text{DWBA})/d\sigma(\text{PWBA})$ is, we believe, a good example of the insensitivity of the partial-wave analysis at low-momentum transfer to different models.

Nevertheless, the sensitivity of the distortion ratio is evident in Fig. 2 where the transition skin thickness, t_{tr} , is varied.^{11,12} t is taken from elastic electron scattering. The Coulomb-distortion ratio f_e is computed with $t_{tr}/t = 0.80, 1.00$, and 1.20 , and with another model, $J_N = \rho_0 Y_{111}^{M*}$, where ρ_0 is given by (4). Since the radial part of $J_N + \nabla \times \mu_N$ is needed to compute (2) and yet the best values of the transition operator come from electron scattering, one is faced with an iterative procedure in determining the transition nuclear form factor.⁹ The accuracy of the experiments needed to make such an iteration is not yet clear.

The remaining features of the Duke calculation have been described in detail, and in the very low-energy domain discussed by us previously.⁴ In the calculations presented here, $M1$ transitions are calculated for $Z \leq 14$ and $E_0 \leq 70$ MeV, where 10 partial waves are found to be sufficient. By repeating the calculation with $Z=0$, one computes the cross section in the normal Born approximation the hard way, i.e., by synthesizing $\exp(i\mathbf{k} \cdot \mathbf{r})$ and $\exp(i\mathbf{k}' \cdot \mathbf{r})$ from their partial waves.

This provides the best check of the computer program. Tuan *et al.* have made this comparison with the analytic form of the Born-approximation cross section.⁸ We call the $Z=0$ result the plane-wave Born-approximation cross section $d\sigma(\text{PWBA})$, in order to contrast it with $d\sigma(\text{DWBA})$. Tuan *et al.*⁸ call the $Z=0$ result, the partial-wave Born approximation for reasons that are clear.

In Sec. 3 the results of our computations are reported as $d\sigma(\text{DWBA})/d\sigma(\text{PWBA})$, which we call the distortion ratio.^{4,9} The separability of the final cross section into a product of electron and nuclear transition elements is a result of the first-order Born-approximation prescription. Schucan has investigated this question of the decomposition of the inelastic electron scattering cross section from an examination and extension of Cutler's second-order Born-approximation calculation. He has examined the model dependency of the result, as well, and the reader is referred to his paper for an excellent discussion.⁷ He finds for electric transitions that

$$d\sigma(\text{DWBA})/d\sigma(\text{PWBA}) = K_L^2(E_0, q; Z, \rho_0; \rho_L), \quad (5)$$

where $K_L^2 = 1 + \alpha Z \rho_L$. Analytical expressions are given for $E0$ and $E2$ transitions by reformulating Cutler's investigation of Coulomb-distortion effects in the second-order Born approximation. Since analytical expressions are not available for magnetic dipole transitions, we will develop some expressions from the systematics of our computer results as $d\sigma(\text{DWBA})/d\sigma(\text{PWBA})$ versus E_0 and versus Z for $k \leq E_0 \leq 70$ MeV.

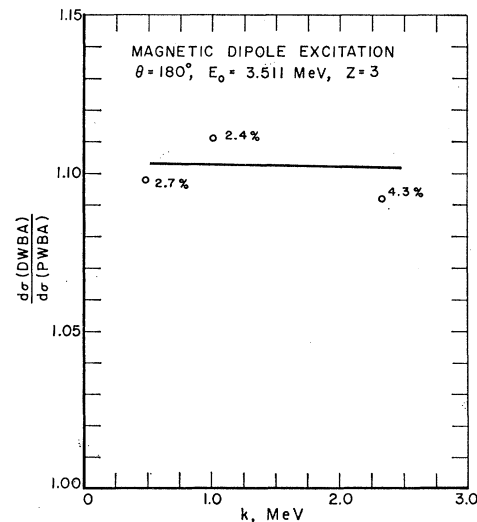


FIG. 4. Calculated $M1$ distortion ratio versus nuclear excitation energy k is presented. The calculation is for 3-MeV electrons (kinetic energy) scattered from ${}^3\text{Li}$ at 180° . The percentages on the computed points are one-standard-deviation errors in $d\sigma(\text{DWBA})/d\Omega$ giving the amount of convergence of the last six partial waves of the transition amplitude squared [Eq. (18) of Ref. 8 and p. 266 of Ref. 12].

¹¹ M. Duguay, C. Bockelman, T. Curtis, and R. Eisenstein, *Phys. Rev.* **163**, 1259 (1967).

¹² J. Ziegler, Atomic Energy Commission Report No. TID-4500, Yale-2726E-49, 1967 (unpublished).

3. RESULTS

A. Very Low Energy

Figures 3–5 present the results of the partial-wave analysis giving Coulomb-distortion effects in $M1$ transitions for low- Z nuclei which are excited by near-threshold energy electrons.

From the linearity of the distortion ratio versus atomic number in Fig. 3,^{7,13} one can deduce an analytical expression for $M1$ electroexcitation at $E_0 = 3.511$ MeV, $k = 2.325$ MeV, and $\theta = 180^\circ$:

$$d\sigma(\text{DWBA})/d\sigma(\text{PWBA}) = (1 + \alpha Z\beta), \quad (6)$$

where $\beta = 4.4$ and α is the fine-structure constant. Figure 4 shows the insensitivity of the distortion ratio on k for $Z = 3$, with E_0 and θ the same as in Fig. 3 for $M1$ excitation. The particular excitation energy $k = 2.325$ MeV was chosen, because in the $D(e, e')np$ problem,¹⁴ it is near the peak of 1S resonance, i.e., ~ 100 keV in the $n-p$ system. Since $M1$ electroexcitation for $E_0 > k$ is only observable at large angles of $\theta > 150^\circ$ ¹⁵ (because of a large bremsstrahlung radiation tail), we note that the distortion ratio may increase by $\sim 10\%$ at 150° compared to 180° . In general, for $E_0 \gtrsim 5$ MeV,

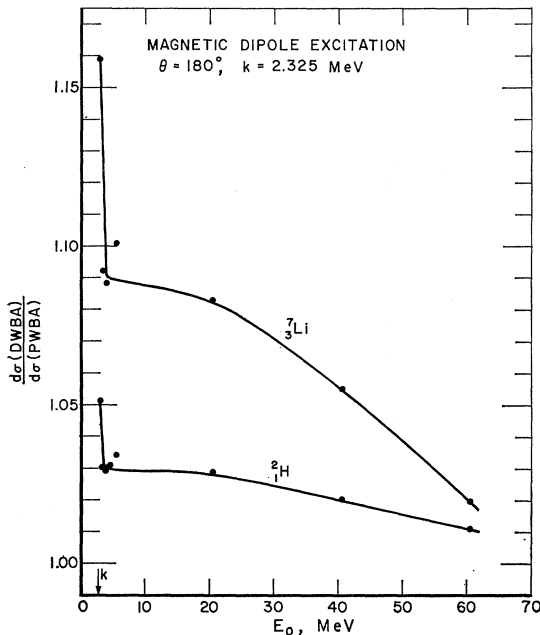


FIG. 5. Calculated $M1$ Coulomb-distortion ratio versus electron energy for $Z=1$ and 3 , $\theta=180^\circ$, and $k=2.325$ MeV is presented. The rapid change in f_c near $E_0=5$ MeV results from strong interference of the $l=0$ and $l=1$ partial waves. The linearity of f_c with Z at a given electron energy is observed here as well as in Figs. 3 and 6.

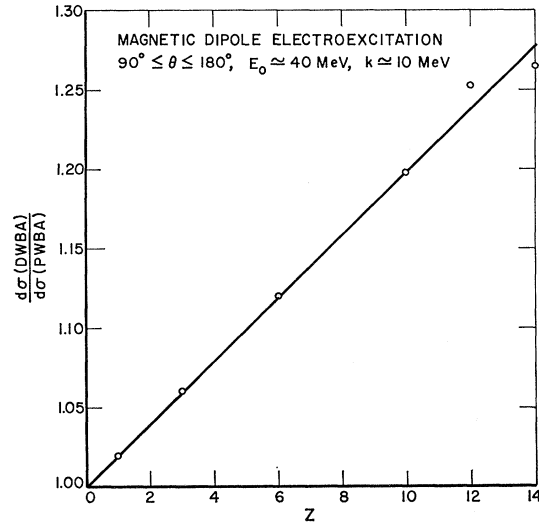


FIG. 6. The ratio $d\sigma(\text{DWBA})/d\sigma(\text{PWBA})$ versus atomic number for $M1$ excitation at $E_0 \approx 40$ MeV, $k \approx 10$ MeV, and $90^\circ \leq \theta \leq 180^\circ$ is linear and $f_c = 1 + 2.72 Z\alpha$. Computations are valid for E_0 (39.0–41.5 MeV) and k (10.0–15.1 MeV). The particular insensitivity of $f_c(M1)$ with angle for $\theta > 90^\circ$ at $E_0 \approx 40$ MeV is not general.

use of the 180° results in Fig. 1 for scattering angles greater than 150° may incur a 1–2% net error.

The dependence on incident energy from threshold to 60 MeV for $Z=1$ and 3 is presented in Fig. 5. Three regions of distortion are visible: threshold to 5 MeV where the s -wave interaction dominates the electron wave-nucleus interaction (e.g., see Figs. 2 and 3 in Ref. 4); $5 < E_0 < 20$ MeV, where s and p waves are important; and $20 < E_0 < 60$ MeV, where the p waves dominate the s - and d -wave contributions. Since the partial-wave amplitudes add coherently, the final distortion ratio results from a strong interference of $l=0, 1, 2, \dots$. The incident electron energy determines the important partial waves while the multipolarity of the nuclear transition and electron scattering angle determine the nature of the mixing, i.e., constructive or destructive interference, or possibly incoherent addition.

B. Low Energy, $30 < E_0 < 70$ MeV

Figure 6 exhibits the same linearity as in Fig. 3 for $d\sigma(\text{DWBA})/d\sigma(\text{PWBA})$ versus Z at $E_0 \approx 40$ MeV, $k \approx 10$ MeV, and $90^\circ \leq \theta \leq 180^\circ$.¹⁶ Using Eq. (6), one finds $\beta = 2.72$. The electron and excitation energies selected in Fig. 6 are in a region where several groups¹⁷ have measured giant $M1$ transition form factors; they are ^{12}C ($k = 15.1$ MeV), ^{20}Ne (11.25 MeV), ^{24}Mg (10.70 MeV), and ^{28}Si (11.42 MeV), as well as ^6Li (3.56 MeV) and ^{10}B (7.477 MeV). The results in Fig. 6 are insensitive to E_0 (39.0–41.5 MeV) and to k (10.0–15.1 MeV).

For electroexcitation of the 15.1 MeV, $I=1^+$, $T=1$

¹³ W. McKinley, Jr., and H. Feshbach, Phys. Rev. **74**, 1759 (1948).

¹⁴ G. Peterson and W. Barber, Phys. Rev. **128**, 812 (1962).

¹⁵ B. Chertok and E. Booth, Nucl. Phys. **66**, 230 (1965).

¹⁶ Figure 6 appears in Ref. 6 and is included here for completeness.

¹⁷ See Refs. 1–4 of Ref. 6.

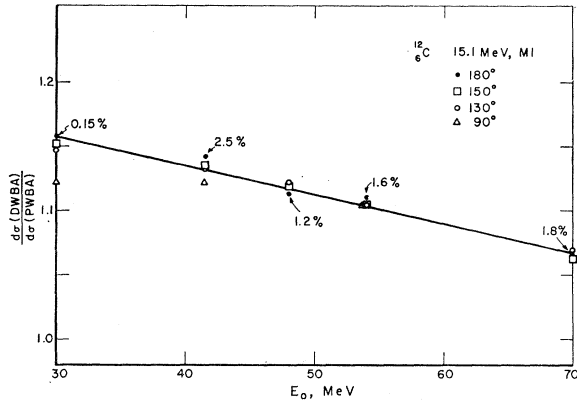


FIG. 7. $M1$ distortion ratios versus E_0 and θ are presented for the ^{12}C giant- $M1$ transition at 15.1 MeV. Percentages on five of the computed points are convergence errors as discussed in the caption of Fig. 4. Energies and angles selected span the experimental data used in Fig. 8.

state of ^{12}C , the dependence of the distortion ratio on both incident electron energy and angle of scatter is shown in Fig. 7. The linear behavior of the ratio versus E_0 is observed for other nuclei; specifically ^{10}B and ^{28}Si have been checked. By linear extrapolation, one observes that $d\sigma(\text{DWBA}) = d\sigma(\text{PWBA})$ at ≈ 108 MeV for ^{12}C for $\theta > 90^\circ$, while for ^{28}Si ($k = 11.42$ MeV) the same linearity with E_0 leads to no distortion at ≈ 67 MeV for $\theta > 150^\circ$ and ≈ 81 MeV for $\theta = 105^\circ$.

Both the ^{12}C calculations presented in Fig. 7 and the ^{28}Si systematics show some sensitivity versus backward scattering angle. For ^{12}C one observes that $d\sigma(\text{DWBA})/d\sigma(\text{PWBA}) \neq f(\theta)$, $\theta > 90^\circ$ for $E > 40$ MeV while for ^{28}Si $M1$ electroexcitation an opposite behavior is observed. The distortion ratio curves versus E_0 for ^{28}Si diverge for $E_0 > 40$ MeV so that at 60 MeV $f_c(105^\circ) = 1.142$ and $f_c(\theta > 150^\circ) = 1.070$. This angular dependence of the distortion is evident in Figs. 1 and 2 for ^{12}C and ^{28}Si , respectively, and is observed in Drechsel's calculations for $Z = 28$.

$M1$ radiative widths for strong transitions in ^{10}B , ^{12}C , ^{26}Mg , and ^{28}Si are presented in Table I.¹⁸⁻²³ The widths come from extrapolations to $q^2 = k^2$ of inelastic electron scattering data analyzed in the DWBA as in Fig. 8 and in Fig. 2 of Ref. 6. The one-standard-deviation error includes the uncertainty in our judgment which is introduced by the model dependency of the Coulomb corrections.

¹⁸ E. Spamer, Z. Physik **191**, 24 (1966).

¹⁹ S. Skorka, J. Hertel, and T. Retz-Schmidt, Nucl. Data **2A**, 347 (1966).

²⁰ G. A. Peterson, Phys. Letters **25B**, 549 (1967). Radiative widths are reported from electron scattering for both ^{12}C and ^{13}C for the 15.1-MeV states, $\Gamma_0 = 36 \pm 3$ eV and 25 ± 7 eV, respectively.

²¹ H. Kuehne, P. Axel, and D. Sutton, Phys. Rev. **163**, 1278 (1967).

²² W. Bendel, L. Fagg, R. Tobin, and H. Kaiser, Phys. Rev. **173**, 1103 (1968).

²³ H. Liesem, Z. Physik, **196**, 174 (1966).

4. DISCUSSION

A. ^{12}C

Reanalysis of the inelastic electron scattering measurements from the 15.1 MeV ^{12}C state is presented in Fig. 8. The 15.1-MeV state of ^{12}C was first investigated with electroexcitation by Barber's group at Stanford using near 180° electron scattering.²⁴ Since most of the measurements of inelastic electron scattering are normalized to the elastic electron scattering peak, one must make Coulomb-distortion corrections to both inelastic and elastic plane-wave cross sections which are included in the original analysis. Thirty-four partial waves were used in these elastic scattering calculations.²⁵

The Coulomb corrections to the measurements cited in Fig. 8 come mainly from the distortion ratios shown in Fig. 7, but include Coulomb corrections to the elastic cross sections varying from 1.06 at $E_0 = 34.9$ MeV, $\theta = 92.9$ ($q^2 = 0.043$ fm $^{-2}$) to 1.00 at $E_0 = 55.0$ MeV, $\theta = 130^\circ$ ($q^2 = 0.186$ fm $^{-2}$). The Darmstadt²⁶ and Orsay²⁷ data were further adjusted using the recent rms charge radius, $a = 2.42$ fm, instead of $a = 2.50$ fm which those groups used in the original data analysis. The photon point at $q^2 = k^2$ in Fig. 8 is from the photon scattering and photon self-absorption measurements of Kuehne, Axel, and Sutton using $\Gamma_0/\Gamma = 0.96$.²¹

From our extrapolation of the inelastic electron scattering data to $q^2 = k^2$, the radiative width of the 15.1-MeV state in ^{12}C is 32.6 ± 3.5 eV.^{6,28} This value is

TABLE I. Radiative widths of magnetic dipole transitions.

	k (MeV)	$\Gamma_0(\text{PWBA})$ (eV)	$\Gamma_0(\text{DWBA})$ (eV)	Photon self-absorption Γ_0
^{10}B	7.477	12 ± 2^a	11.0 ± 2.2^b	
^{12}C	15.1	$36 \pm 3^{c,d}$	32.6 ± 3.5	37 ± 5 eV e,e
^{26}Mg	10.63	$9.1_{-1.7}^{+2.0}$ f	6.8 ± 2.5	
^{28}Si	11.42	$32.4 \pm 4.5^{g,h}$	25.7 ± 3.9	$23 \pm 4^{e,c}$

^a Reference 18.

^b Results in this column are from the present analysis.

^c Reference 19.

^d Reference 20.

^e Reference 21.

^f Reference 22.

^g Reference 23.

²⁴ J. Goldemberg, W. Barber, F. Lewis, Jr., and J. Walecka, Phys. Rev. **134**, B1022 (1964), and Refs. 5 and 6 therein; R. Edge and G. Peterson, *ibid.* **128**, 2750 (1962).

²⁵ C. Fischer and G. Rawitscher, Phys. Rev. **135**, B377 (1964).

²⁶ F. Gudden, Phys. Letters **10**, 313 (1964). The reported value $\Gamma_0 = 34.4$ eV $\pm 10\%$ was deduced assuming that the rms radius $a = 2.50$ fm, for ^{12}C . Use of the recent value 2.42 fm increases the Γ_0 somewhat.

²⁷ B. Dudelzak and R. Taylor, J. Phys. Radium **22**, 544 (1961).

²⁸ The reduced nuclear transition probability plotted in Fig. 8 and the radiative width are connected by $B(M1, k, \downarrow) = (9/16\pi)(k/\hbar c)^{-2}\Gamma_0/c\hbar c$.

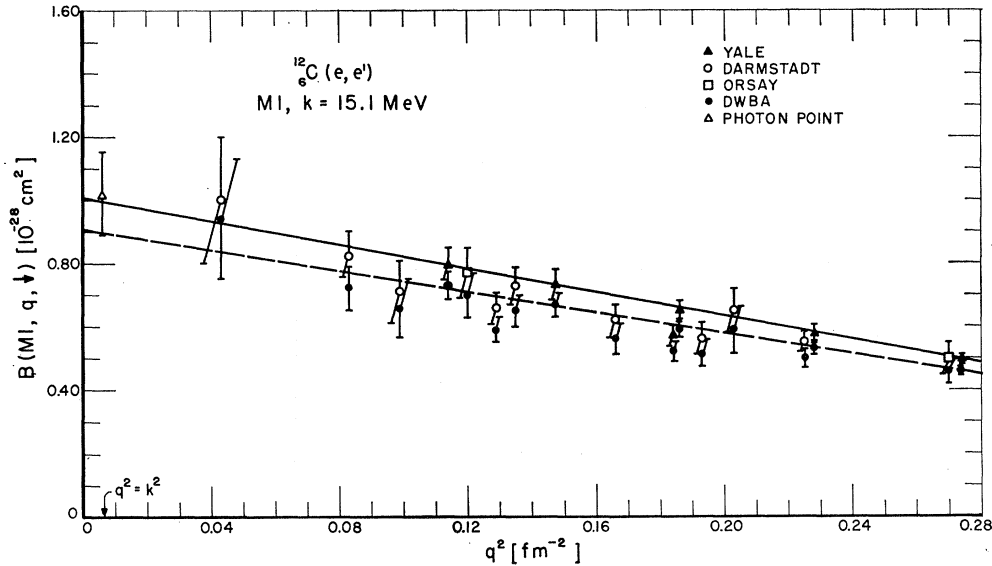


FIG. 8. Reduced nuclear transition probability versus the momentum transfer squared is presented for the 15.1-MeV $M1$ transition in ^{12}C . The electron scattering data are from three laboratories. \blacktriangle : Ref. 20; \circ : Ref. 26 and an unpublished compilation; and \square : Ref. 27. The photon point is from Ref. 21. Darmstadt points at $q^2=0.12, 0.164, 0.170,$ and 0.228 fm^{-2} are omitted so that points analyzed both in the PWBA and DWBA can be displayed. Three data points from near 180° electron scattering of the Stanford group are omitted for the same reason. Each electron data point is reanalyzed using Coulomb-distortion corrections to both the elastic and inelastic scattering peaks. The latter corrections are from Fig. 7 and the Coulomb-distortion-corrected data points are shown as \bullet . The radiative width from extrapolation to the photon point $q^2=k^2$ is $\Gamma_0=32.6\pm 3.5 \text{ eV}$ (Ref. 6) which is 11% smaller than the width from the PWBA analysis.

11% smaller than the width extracted from the Yale measurements using an analysis with plane waves.²⁰ The photon scattering and self-absorption value is $\Gamma_0=37\pm 5 \text{ eV}$.²¹ As noted earlier, the inconsistencies (in a precision sense) among laboratories in the $^{12}\text{C}(e, e')$ data for the 15.1-MeV state indicate the need for caution in using our Coulomb-corrected radiative width.⁶ For example, with a least-square fit to all of the data, one obtains $\Gamma_0=34.6 \text{ eV}$ with a second-order fit, $B=a+bq^2+cq^4$, compared to 29.2 eV from a first-order fit to the data. The larger value of the radiative width results from the measurement at $q^2=.043 \text{ fm}^{-2}$, while the smaller value of Γ_0 results mainly from the Darmstadt data, which are more plentiful, and hence weighted more in the least squares fit. In a precision experiment a state at 14.7 MeV and possibly one at 15.5 MeV in ^{12}C , could influence the experimental results.²⁹

The magnetic dipole strength of the ground-state radiative transition from the $I=1^+, T=1, 15.1 \text{ MeV}$ state in ^{12}C has important roles in the conserved vector current theory,³⁰ in particle-hole calculations in the $1p$ shell,³¹ and in the interpretation of photon self-absorption and scattering measurements.²¹ We briefly review the role of the transition magnetic moment of ^{12}C as the meeting ground between experiment and the CVC theory.

²⁹ S. Penner (private communication).

³⁰ C. Wu, Rev. Mod. Phys. **36**, 618 (1964).

³¹ T. Donnelly, J. Walecka, I. Sick, and E. Hughes, Phys. Rev. Letters **21**, 1196 (1968).

B. ^{12}C and CVC Test

The CVC theory of weak interactions uniquely gives a relationship between the weak vector form factors and the isovector electromagnetic form factors.³² β decay and electromagnetic transitions can be connected in spin-isospin flip transitions since the interaction Hamiltonians are

$$(H_{\text{int}})_{\gamma} = (-e/2M) \boldsymbol{\mu} \cdot \nabla \times \mathbf{A}, \quad (7)$$

$$(H_{\text{int}})_{\beta^{\pm}} = (-g/\sqrt{2}M) \boldsymbol{\mu} \cdot \nabla \times \mathbf{J}^{(\beta)} \text{ weak}, \quad (8)$$

where $\boldsymbol{\mu} = \boldsymbol{\mu}_p - \boldsymbol{\mu}_n$.³⁰ Thus, the pionic clouds which are the source of giant $M1$ electromagnetic transitions in self-conjugate nuclei must also appear in vector β decay.

In the $T=1$ triad, ^{12}B , ^{12}C , and ^{12}N , the $T_3=0$ member at 15.1 MeV in ^{12}C makes a strong radiative transition to ground, while ^{12}B and ^{12}N both β decay in allowed Gamow-Teller transitions, $1^+ \rightarrow 0^+$, to the ^{12}C ground state. Measurement of the $M1$ radiative width determines $\boldsymbol{\mu}$ the transition isovector magnetic moment, since

$$|\langle I=1, T=1 | \boldsymbol{\mu} | 00 \rangle|^2 = \text{const} \times B(M1, k). \quad (9)$$

The interference in β decay, $^{12}\text{B}^{\beta^-} \rightarrow ^{12}\text{C}$ and $^{12}\text{N}^{\beta^+} \rightarrow ^{12}\text{C}$, between the predominant axial vector and forbidden vector coupling can be measured as a deviation in the shape of the β -ray energy spectrum. Essentially this determines $\boldsymbol{\mu}$ in Eq. (8) from the weak interaction.

³² M. Gell-Mann, Phys. Rev. **111**, 362 (1958).

The ratio of the two shape factors, $A = a^-(^{12}\text{B})/a^+(^{12}\text{N})$, is $(1.07 \pm 0.24)\%$ from β -decay experiments³⁰ and $(0.91 \pm 0.17)\%$ from CVC theory with $\Gamma_0 = 37 \pm 5$ eV.²¹ With the new value, $\Gamma_0 = 32.6 \pm 3.5$ eV, from inelastic electron scattering, one obtains $A = (0.85 \pm 0.17)\%$. However, the present electron scattering experiments do not rule out a $\Gamma_0 = 29.2$ eV for 15.1 ^{12}C in which case $A = (0.81 \pm 0.17)\%$. The consistency between the measured Γ_0 in ^{12}C and the ratio of the shape factors, is essentially a determination of the μ in (7) and (8) from γ -ray or electron scattering measurements and independently from β -ray measurements assuming the universality of the electric charge.

We conclude this section with a recommendation for future work. In view of the importance of the radiative width of the 15.1-MeV ^{12}C state as discussed above and elsewhere, it is recommended that inelastic electron scattering measurements be made with high resolution, 0.1% at low q^2 , e.g., 0.020, 0.025, 0.040, 0.060, and 0.080 fm^{-2} . This should conclusively determine Γ_0 and give the groups using the method of the photon self-absorption, a radiative width with which to test their method and assumptions. Further, it is hoped that such measurements will provide a framework to remove any model dependency of the Coulomb corrections such as that observed in Figs. 1 and 2.

C. Deuteron Electrodintegration

180° inelastic electron scattering induces a spin-isospin $M1$ transition from the bound two-nucleon state to the continuum, $^3S_1 \rightarrow ^1S_0$. Meson systems with even G parity such as $\pi\pi$, $\omega\pi$, and $\rho\eta$, which produce electromagnetic transition currents have been invoked to explain the discrepancies between experiment and bare nucleon theory in the impulse approximation at $q_\mu q^\mu \simeq 10^{-4}$, -0.16 , -0.30 , and -4 to -10 fm^{-2} .³³

Plane waves were used for the electrons in the initial and final states. The correction to $d\sigma(\text{PWBA})$ from the distortion of the plane waves in the nuclear Coulomb field of the deuteron is given in Fig. 5. As already mentioned in Sec. 3 A, three regions of distortion are visible. These are threshold to ~ 5 MeV, $5 < E_0 < 20$ MeV, and $20 < E_0 < 60$ MeV. The variation with increasing E_0 can be understood as an interference phenomenon as higher l waves become important. Ten partial waves were used in the calculations and the excitation energy $k = 2.325$ represents 100 keV (near the 1S_0 peak) in the n - p system. The ratio $d\sigma(\text{DWBA})/d\sigma(\text{PWBA})$ is 1.051 at $E_0 = 3.011$ MeV, 1.029 at 5.00 MeV, 1.028 at 20.00 MeV, 1.020 at 40 MeV, and 1.011 at 60 MeV. An extrapolation of the curve to the ratio = 1.00 occurs at ≈ 80 MeV.

The first measurements of electrodisintegration of the deuteron, where the momentum spectrum of the outgoing electron was observed, were those of Peterson and Barber at $E_0 = 41.5$ MeV, $\theta = 177.1^\circ$.¹⁴ The accuracy

of the measurements was $\sim \pm 10\%$ near the 1S_0 resonance and they were in agreement with the first Born-approximation calculation of Jankus.³⁴ The theory of Jankus neglected exchange currents, used a Hulthén wave function for the 3S_1 ground state and in later versions, included final-state interactions in the 1S_0 wave function. This theory has been superseded by an impulse-approximation calculation of Adler which includes meson exchange currents (mainly π - γ - π), and uses Partovi and Reid wave functions for the ground state and standard phenomenology for the 1S_0 .³⁵ For Peterson's measurements, this calculation predicts that 2–4% of the $M1$ electrodisintegration cross section is due to meson currents, and it gives agreement with the much higher q^2 measurements at $q^2 = -6$ and -8 fm^{-2} . Later measurements³⁵ of $D(e, e')np$ at 54 and 70 MeV and 180° were in sharp disagreement with those of Peterson *et al.*, but recent measurements³⁶ at 38, 70, and 90 MeV at $\theta = 155^\circ$ are in agreement with the earliest measurements.

Coulomb corrections and meson exchange currents are small effects in disintegration of the deuteron by low-energy electrons. Both effects appear to be less than 5% of the dominant spin-flip cross section. Measurements of inelastic electron scattering near 180° with accuracies significantly exceeding 10% are difficult. In this light we note that radiative capture by hydrogen of thermal neutrons, $^1\text{H}(n, \gamma)^2\text{H}$ is equivalent to inelastic electron scattering on the mass shell, $q^2 = k^2 \simeq 10^{-4}$ fm^{-2} . The total cross section at $v_n = 2,200$ m/sec has been accurately determined, $\sigma_a(^1\text{H}) = 334.2 \pm 0.5$ mb. Theoretically, the near zero energy, $E_{\text{c.m.}} = 1/80$ eV, permits use of effective range theory in determining the $M1$ radial overlap integral. Indeed, the Bethe-Longmire effective-range approximation in modern form predicts 302 ± 4 mb for the $n\bar{p}$ radiative capture cross section. It is significant, then, that $^1\text{H}(n, \gamma)^2\text{H}$ at $q^2 \simeq 10^{-4}$ fm^{-2} may be more suitable for determining meson exchange effects than from $^2\text{H}(e, e')np$ for $E_0 < 200$ MeV.³⁷

5. CONCLUSIONS

The distortion of electrons in the static nuclear Coulomb field is appreciable even in light nuclei for inelastic electron scattering. Partial-wave-analysis computations have been made in the electron energy range $k < E_0 < 70$ MeV.

This study of Coulomb-distortion effects has been focused on $M1$ induced transitions for two reasons. Firstly the systematics of Coulomb-distortion effects in $M1$ electroexcitation have not been presented, whereas results for important electric transitions have been systematized both from extensive partial-wave

³⁴ V. Jankus, Phys. Rev. **102**, 1586 (1956).

³⁵ J. Goldemberg and C. Schaerf, Phys. Letters **20**, 193 (1966).

³⁶ L. Katz, G. Ricco, T. Drake, and H. Caplan, Phys. Letters **28B**, 114 (1968).

³⁷ R. Adler, B. Chertok, and H. Miller (to be published).

³³ R. Adler, Phys. Rev. **169**, 1192 (1968); **169**, 1192 (E) (1968).

analysis^{11,38} and from analytic expressions for f_c , Eqs. (1) and (5).⁷ Secondly, the class of physical problems which can be studied by $M1$ isovector transitions in light nuclei is, in our view, quite meaningful. This is illustrated by the discussion presented on the CVC test in the $A=12$ isobaric triad and on meson exchange currents in electromagnetic processes in the two-nucleon problem. Coulomb effects during inelastic electron scattering have an important bearing on these problems.

The dependency of the distortion ratio f_c defined in Eq. (1) on the assumed nuclear transition currents is the critical reservation about the results presented here. Allowances have been made in Table I for this uncertainty. Progress is being made on parametrizing the transition currents.¹⁰ Finally we must mention that the more basic problems associated with the DWBA

³⁸ C. Toepffer and D. Drechsel, *Z. Physik* **210**, 423 (1968).

calculation for inelastic electron scattering have been defined by Drechsel.⁹

ACKNOWLEDGMENTS

The author wishes to thank Dr. J. W. Motz for continued hospitality extended to our group at the National Bureau of Standards. Dr. E. C. Booth suggested some time ago the usefulness of a systematic study of Coulomb-distortion effects for inelastic electron scattering. W. T. K. Johnson is cited with appreciation for his efforts with the Duke program and the computations presented here. The calculations were done at the National Bureau of Standards and Harry Diamond Laboratories' Computation Centers. B. Levy and D. M. Skopik provided assistance on the elastic electron scattering and ¹²C computations, respectively. Finally, Dr. D. Drechsel is thanked for a critical reading of the manuscript.

Decoupling Parameter in Light Nuclei*

K. L. BHATIA AND N. DE TAKACSY

Institute of Theoretical Physics, McGill University, Montreal, Quebec, Canada

(Received 9 June 1969)

The approximate-projection method of Das Gupta and Van-Ginneken is extended to include the calculation of the decoupling parameter for $K=\frac{1}{2}$ bands. The method is tested on the first positive- and negative-parity bands of ¹⁹F and is found to give good results even when the strong-coupling model seems to fail. The validity of the formula for the decoupling parameter given by the strong-coupling model is explored.

1. INTRODUCTION

IN a previous paper, Das Gupta and Van Ginneken¹ have developed an approximate method² for calculating the energies of states in a rotational band which avoids the problem of exact projection from an intrinsic, deformed, Hartree-Fock determinant.³ The method assumes a rotational structure, but departures from the $J(J+1)$ rule were also studied and in particular, the possibility of decoupling in $K=\frac{1}{2}$ bands was included in the formalism. In this case, the decoupling parameter was calculated by the Bohr-Mottelson prescription.⁴ It is the purpose of this paper to fully

incorporate the calculation of the decoupling parameter into the formalism of the method of approximate projection. The notation in the rest of the paper follows closely that of Ref. 1.

2. METHOD OF APPROXIMATE PROJECTION

The states $|\Psi_{J\frac{1}{2}}\rangle$ in the band are in principle obtained by angular momentum projection from an intrinsic determinant $|\Phi_{\frac{1}{2}}\rangle$ and their energies are assumed to follow a rotational sequence:

$$|\Phi_{\frac{1}{2}}\rangle = \sum_J a_J |\Psi_{J\frac{1}{2}}\rangle, \quad (1)$$

$$E^J \equiv \langle \Psi_{J\frac{1}{2}} | H | \Psi_{J\frac{1}{2}} \rangle = E_0 + AJ(J+1) + aA(-)^{J+1}(J+\frac{1}{2}). \quad (2)$$

Here, E_0 is the band head, $A = \hbar^2/2\mathfrak{I}$, where \mathfrak{I} is the moment of inertia, and a is the decoupling parameter. We can then define a pseudo-Hamiltonian

$$\mathfrak{H} = E_0 + AJ^2 + aAJ, \quad (3)$$

which is required to have the same intraband matrix elements as the true Hamiltonian H . In Eq. (3), J is

* Work supported in part by the National Research Council of Canada.

¹ S. Das Gupta and A. Van Ginneken, *Phys. Rev.* **164**, 1320 (1967); S. Das Gupta and M. Harvey, *Nucl. Phys.* **A94**, 602 (1967).

² Similar methods have been proposed previously: T. H. R. Skyrme, *Proc. Phys. Soc. (London)* **70**, 433 (1957); R. E. Peierls and J. Yoccoz, *ibid.* **70**, 383 (1957); J. Yoccoz, *ibid.* **70**, 388 (1957).

³ G. Ripka, in *Advances in Nuclear Physics*, edited by M. Baranger and E. Vogt (Plenum Publishing Corp., New York, 1968).

⁴ A. Bohr and B. Mottelson, *Kgl. Danske Videnskab. Selskab, Mat.-Fys. Medd.* **27**, 16 (1953).